 doi:10.20944/preprints202209.0267.v1

Article

Development of a Technique for Estimating the *Moniliophthora Roreri* Spore Loads of Cacao Fields

Diana L. Jiménez-Zapata[1], Manuela Quiroga-Pérez[1], Manuela Quiroz-Yepes[1], Alejandro Marulanda-Tobón[1], Javier C. Álvarez[1,2*] and Sandra Mosquera-López[1,2]

[1] Division of Natural Systems and Sustainability, School of Applied Sciences and Engineering EAFIT University, Medellín, Colombia
[2] CIBIOP research group, School of Applied Sciences and Engineering, EAFIT University, Medellín, Colombia
* Correspondence: Javier C. Álvarez, jcorre38@eafit.edu.co

Abstract: Frosty pod rot, caused by *Moniliophthora roreri*, is the most damaging disease of cacao in Latin America. However, to better comprehend its epidemiology, we must understand its dissemination and proliferation. Still, we ignore how loads of *M. roreri* spores fluctuate across growing seasons since we lack a reliable technique to quantify *M. roreri* spores in the fields. Therefore, we developed a method that uses a spore trap to capture *M. roreri* spores and qPCR to quantify them. This study demonstrated that this technique could quantify 3.9 x10^4 *M. roreri* spores with a 95 % confidence level. However, it could not differentiate between *M. roreri* and its close relative, *M. perniciosa*. Despite this limitation, we could detect and quantify *Moniliophthora* spores from environmental samples taken from a cacao field. This technique can help the phytopathologist address studies more accurately in disseminating cacao pathogens.

Keywords: spore trap; qPCR; Moniliasis; *Theobroma cacao*; Frosty pod rot

1. Introduction

Frosty pod rot (FPR), caused by the basidiomycete *Moniliophthora roreri,* is the most prevalent and severe cacao disease in Latin America [1]. This disease causes production losses between 16 % and 100 % depending on the growing region and agronomic factors [1–3]. In Colombia, FPR causes 40 % production losses, but some plantations can lose their entire production [4]. FPR exclusively affects the cacao pods. It begins as chlorotic spots on the pod's surface, which turn dark brown as the disease progress. In severe diseases, brown spots grow, covering the pod's surface. Then, the pod turns white and powdery as *M. roreri* mycelia, and spores colonize its surface [2,5]. These spore-covered pods can carry about seven billion spores, each capable of initiating a new infection. Understanding how *M. roreri* environmental spore loads vary in time and space is critical for its epidemiology and for designing control strategies to mitigate its losses [6]. However, only a handful of studies have measured *M. roreri* spore loads or evaluated their dissemination patterns [2,5–9]. Also, these evaluations are inconclusive, and half are nearly three decades old [5,7,8].

Despite these limitations, the literature has proven that climatic variables influence the *M. roreri* environmental spore loads. Therefore, they change in time and space at different scales [3,5,6,8]. On a small scale, the mist, wind, and rain are critical as they move *M. roreri* spores away from the inoculum source (i.e., sporulated pod) [10]. The spore load and FPR incidence decrease with the distance. However, they do not fall to zero as they plateau at a certain distance and remain at low levels [5,7]. The literature is inconclusive about the distance at which the spore load and FPR incidence *plateau*. Some studies suggest more than one kilometer and others less than 375 m from the inoculum source [4,5,7]. The literature is also unclear on whether the spore loads or FPR incidence *will drop to zero at farther distances.* Despite these uncertainties, the literature agrees that the low *M. roreri*

 doi:10.20944/preprints202209.0267.v1

spore loads remaining in plantations after plateauing constituted a background inoculum ready to initiate an FPR infection under the proper climatic conditions [4,5,7].

In addition, the literature on the daily variation of *M. roreri* spore loads is inconclusive. For example, two studies found the highest concentration of spores around noon [5,8], while another found it at night [11]. On a larger scale, dry months with relatively high temperatures (close to 30 °C) seem relevant as they relate to increased environmental *M. roreri* spore loads and favor their long-distance spread [2,5,8,9,11]. However, the data supporting this assumption is noisy, leading to a weak association [5,8].

Some of the inconsistencies in the literature about the environmental *M. roreri* spore load might derive from the methods used during the evaluations. Most studies used spore traps to collect environmental samples and microscopy to identify and quantify spores [5,8,11]. Other evaluations have used similar approaches in other systems [12]. However, using microscopy for quantifying *M. roreri* spores might not be reliable since these spores vary in shape and size due to their conidiogenetic process [11,13], which might lead to errors. An alternative to microscopy is to grow the trapped spores in culture media and quantify colonies [14]. However, this alternative is time-consuming as *M. roreri* colonies can take weeks to develop [15].

Another fast and reliable alternative to microscopy is quantitative PCR (qPCR). Several studies have coupled spore traps with qPCR to analyze the environmental spore loads of several plant pathogens [16–19], but none have used it for *M. roreri*. A similar technique for estimating the *M. roreri* spore loads would be beneficial since it would facilitate future evaluations characterizing the dynamics of *M. roreri* environmental spore loads. Therefore, this study aimed to develop a method based on spore traps and qPCR to assess the *M. roreri* spore loads in cacao plantations. We designed a spore trap device that captures both *M. roreri* spores in the environment and records climatic variables. We also developed a qPCR protocol to detect and quantify the spores caught in the spore traps. Finally, we evaluated our method in commercial cacao plantations with FPR prevalence.

2. Material and methods

2.1. Fungal strains

The *M. roreri* MR1 and MR2 strains (Table S1) used in this study were isolated from cocoa pods with late FPR symptoms collected from a commercial farm in Barrancabermeja, Colombia (6°54'32.17 "N 73°44'9.37 "O). Specifically, we hit the symptomatic pods over x0.5 potato dextrose agar (PDA, OXOID, England) plates supplemented with kanamycin (Thermo Fisher Scientific, Massachusetts) at 50 µg/ml to release *M. roreri* spores. Plates were incubated at 30 ^{0}C for three days, the time required for the spores to germinate. We used a needle and a stereomicroscope Discovery V12 (Zeiss, Germany) to transfer single-germinated spores to plates containing malt extract agar (MEA) (OXOID). Plates were incubated at 30 ^{0}C for nearly one month, the time required for the colonies to grow and sporulate. Spores were washed off the MEA plates with sterile glycerol (Thermo Fisher Scientific) at 20 % and stored at -80 ^{0}C until needed. The other fungal strains used in these evaluations came from the EAFIT University culture collection (Table S1), and the basidiocarp of the sister species, *Moniliophthora perniciosa,* originated from the same commercial farm as the *M. roreri* MR1 and MR2 strains. All fungal strains, including MR1 and MR2 strains, were activated at 30 ^{0}C in MEA plates.

2.2. Spore traps and spore trap devices

Homemade-spore-trap devices were designed to carry spore traps, comprising 2.5 cm x 6.5 cm sections of crystal-clear adhesive tape (Tesa, Switzerland) attached to microscopy slides with the sticky side facing outwards (Figure 1 and Figure S1). Specifically, the spore-trap devices consisted of an Arduino UNO R3 system with an AVR microcontroller encapsulated in a commercial IP67-ABS box of 18 cm x 8 cm x 7cm. The Arduino UNO

 doi:10.20944/preprints202209.0267.v1

system had an L298N H-bridge motor driver connected to a PWM output, which controlled a 12 V DC 60 rpm geared motor moving 20 cm-long blades carrying the spore traps. These blades were custom-made by additive manufacturing using a 3D printer and polylactic acid.

The spore-trap devices had a Solar-Powered Systems CN3065 for energy harvesting connected to a LiPo 3.7 V 6000 mAh battery and a 1 W 5.5 V Seeed monocrystalline solar panel (170 mA). Also, they had a DS3231 real-time clock (RTC) coupled to the Arduino UNO R3 communicating via an I2C bidirectional bus. SHT31 Sensirion temperature and humidity sensors were attached to the I2C bidirectional bus for collecting environmental data, and the data was stored using a DM3AT micro-SD connector and a 32 GB Sandisk memory.

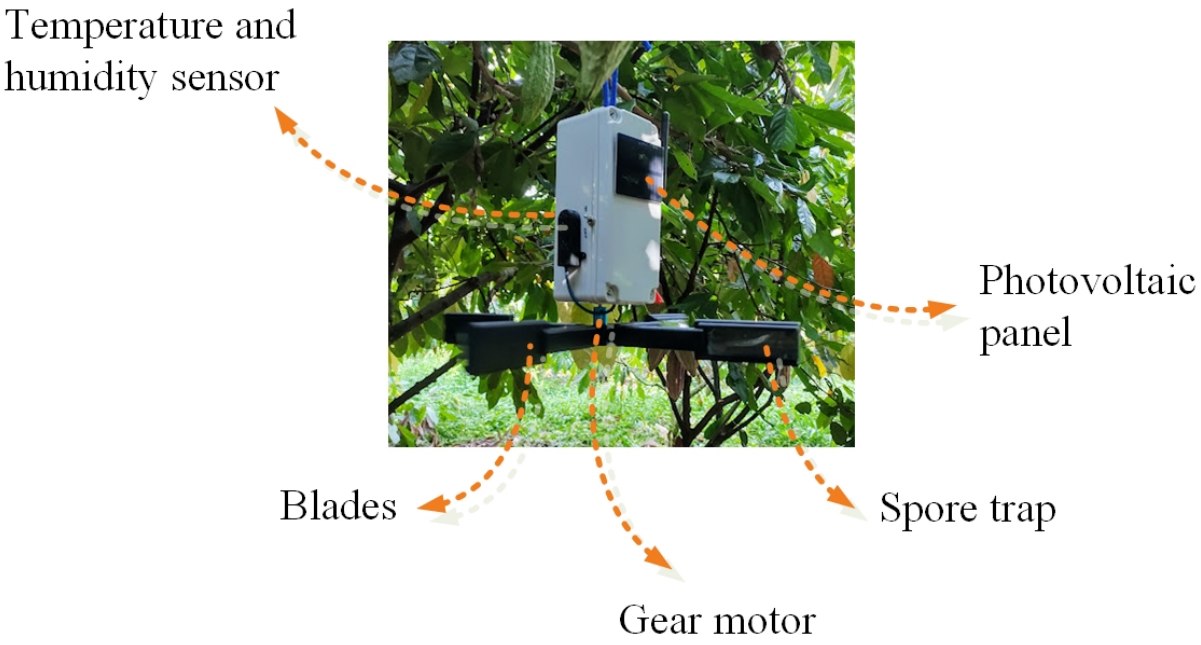

Figure 1. A representative picture of the spore-trap device developed for assessing the *Moniliophthora roreri* spore load in cacao plantations.

2.3. DNA extractions from fungi and spore tramps

For extracting DNA from mycelia, MR1, MR2, and non-*moniliopthora* fungal strains were grown in Sabroud broth cultures (Merck, New Jersey) for 48 h at 200 rpm and 30 ^{0}C. Then, the mycelium was harvested and homogenized using liquid nitrogen, a mortar, and a pestle. The homogenized mycelium was used for DNA extraction with the DNeasy PowerSoil kit (Qiagen, Germany), following the manufacturer's instructions.

For extracting DNA from spore traps and non-trapped *M. roreri* spores, the MR1 strain spores off 15 days-old MEA plates was washed with sterile 0.05 % tween 80 (Merk). Then, the spores were used to make serial dilutions (x 1/10n) with concentrations between 10^{6} spores per ml and 10^{2} spores per ml, using a Neubauer chamber (Boeco, Germany). For non-traped spores, 2 ml of the 10^{6} spore/ml suspension were centrifugated at 4500 rpm for 10 min to collect the spores ($2x10^{6}$ spores). For spore traps, 2 ml of each spore suspension (between $2x10^{2}$ and $2x10^{6}$ spores depending on the spore suspension) were spread on 2.5 cm x 6.5 cm tape sections and allowed to dry. The tape sections were cut into 0.7 cm x 0.7 cm pieces to facilitate the DNA extraction and placed in sterile 50-ml falcon tubes containing Ballotini beads of 4- and 2-mm diameter (~ 3 ml).

 doi:10.20944/preprints202209.0267.v1

Samples were mechanically disrupted six times for 30 sec using a vortex (Labnet S0200 Model VX-200 Vortex Mixer) at maximum speed, with submersion in liquid nitrogen between disruption cycles to avoid DNA degradation. Five ml of lysis buffer, containing 100 mM Tris pH 8.0 **(PanReac, Spain),** 3 M sodium chloride (NaCl) (ProtoKimica, Colombia), 3 % (P/V) cetrimonium bromide (CTAB) (Amresco, Ohio), 20 mM EDTA (**PanReac**), 1 % (P/V) polyvinylpyrrolidone (PVP-40, molecular weight 40,000) (Amresco) and 1 % (V/V) β-mercaptoethanol (Amresco), were added to the disrupted samples. Then, they were incubated at 65 °C for 1 hour. During this incubation, samples underwent additional disruption cycles of 10 sec every 10 min to facilitate spore lysis. An equal volume of chloroform: isoamyl alcohol (24:1) (Sigma-Aldrich, Missouri) was added to the samples and mixed by inversion. Samples were centrifuged for 10 min at 5000 g, and the upper aqueous phase was transferred to new 50-ml falcon tubes. It was added x0.1 volumes of 3 M sodium acetate pH 5.2 (Amresco) and x0.66 volumes of cold isopropanol (ITW Reagents, Illinois) to the samples and mixed the tubes by inversion. Tubes were incubated at -20 °C overnight, and the DNA was precipitated by centrifugation at 15000 g for 10 min. The DNA pellets were washed twice with 3 ml of 70 % ethanol (Sigma-Aldrich) and air-dried. Then, they were resuspended in 50 µl of TE buffer (Bio Basic, Canada) containing 0.05 mg/ml of RNase A (Thermo Fisher Scientific) and incubated at 37 °C for 30 min. The RNase A was deactivated at 65 °C for five min, and the DNA suspensions were kept at -20 °C until used.

We performed a single batch of DNA extraction from mycelia, including all fungal strains, and three independent batches of DNA extractions from non-trapped spores and spore traps. Each DNA extraction batch included two sets of spore traps with all the spore loads (x10n spores between $2x10^2$ and $2x10^6$) and two samples of $2x10^6$ non-trapped spores, resulting in six DNA suspensions for each treatment. The last batch of DNA extraction also included a 100 mg sample of *M. perniciosa b*asidiocarp and three spore traps with environmental samples (refer to Spore evaluation in the field), which were treated as the other samples. The DNA concentration and quality were assessed using a NanoDrop 2000 (Thermo Fisher Scientific spectrophotometer). The DNA integrity was evaluated by electrophoresis using five µl of the extracted DNA in agarose (Amresco) gels at 1 %. Gels were run for 90 minutes at 70 V and visualized using an Enduro GDS gel visualizer (Labnet).

2.4. PCR and qPCR amplification

The primers used in this study targeted regions of the internal transcribed spacer (ITS) of the ribosomal DNA. They included the generic ITS1 and ITS4 primers [20] and the semi-specific Mr_ITSF and Mr_ITSR primers (Table S1). These semi-specific primers targeted ITS regions conserved in *M. roreri* but no other fungi. We identified these regions by aligning ITS sequences of *M. roreri* and other fungi from the GeneBank (Table S1). The alignment and primer design used the global alignment with free end gaps and the primer design functionalities of the Geneious prime application (version 2020.2.3). MAFFT FFT-NS-i (v7.487) was used in the EMBIL-EBI online platform to show the binding sites of Mr_ITSF and Mr_ITSR primers in the alignment of the ITS sequences of *M. roreri* strains MR1 (OM056945), MR2 (OM056946), and MCA2954 (Genbank DQ222927) and the *M. perniciosa* basidiocarp (OM056947).

For PCR amplification, 2 µl of the extracted DNA were used in 20 µl reactions of EconoTaq PLUS (Lucigen, Wisconsin) with the generic (ITS1 and ITS4) or the semi-specific (Mr_ITSF and Mr_ITSR) primers at 0.5 mM. 34 amplification cycles were carried out in a BIO-RAD T100 Thermal Cycler **(**Bio-Rad, California**)** with an annealing temperature of 57 °C and an extension time of 1 min. The remaining conditions followed the manufacturer's specifications. For quantitative PCR (qPCR) amplification, 3 µl of the extracted DNA was used in 10 µl reactions of Universal IT SYBR Green supermix (Bio-Rad) with the semi-specific Mr_ITSF and Mr_ITSR primers at 0.25 mM. The amplification and DNA quantification used the CFX96 real-time system (Bio-Rad) with a PCR program consisting of a

 doi:10.20944/preprints202209.0267.v1

denaturing step of 3 min at 98 °C followed by 34 cycles of 30 sec at 98 °C, **30 sec** at 60 °C, and 15 sec at 77 °C. DNA detection occurred at the end of each cycle, and dissociation curves followed the last cycle.

The specificity of the PCR and qPCR reactions was visually inspected by loading five µl of the amplification products into agarose gels at 1.2 %. Gels were run and visualized as before. A single band in the gels was considered a specific reaction. For the qPCR, single-peak dissociation curves were also considered.

2.5. qPCR characterization and validation

Two qPCR runs were made for each DNA suspension, and each run contained two technical replicates per sample and three non-template controls. The average the threshold cycles (Ct) between the technical replicates was calculated to get a single value per DNA suspension in each qPCR run and 12 Cts for each spore concentration in the spore traps. A technical replicate was excluded from the analysis only when the Ct was above 34 cycles, meaning that the sample failed. In such cases, the remaining replicate was used as the representative value. Both technical replicates failed (Ct > 34 cycles) three times due to technical errors, i.e., two spore traps with $2x10^5$ spores and one spore trap with $2x10^4$ spores. We excluded both replicates from the analysis resulting in a smaller sample size for these spore traps.

Logit approach was used to estimate the qPCR's 90 % and 95 % detection limits [22]. For this evaluation, it was defined a *positive sample* as a sample having a Ct of at least 28 cycles (i.e., five cycles below the 34-cycle cut-off). All non-template controls were negative samples, with Cts of 33 cycles or higher. The probability of *M. roreri* spores to be detected in the spore traps, i.e., return a positive qPCR, was estimated for each spore load (x10n spores between $2x10^2$ and $2x10^6$). Then, the probabilities were fitted into a general linearized model (GLM) using the Logit link function, the binomial error family, and the logarithm with base ten (log10) of the spore load in spore traps as the predictor. The GLM was used to estimate the spore concentrations associated with a 90 % and 95 % probability of yielding a positive qPCR reaction (i.e., 90 % and 95 % detection limits). The probabilities were plotted against the log10 of the spore load using the R library *ggplot2* (version 3.3.3) [23] for visualization. Differences between Ct value means of samples and non-template controls were evaluated using Welch's t-test. This analysis used the R library stat's GLM, predict, and t.test functions (version 4.0.4) [24].

The qPCR efficiency was calculated using the standard- and amplification-curve analyses [25]. For the standard-curve analysis, a linear mixed-effects model (lmer) was used to correlate Ct values with the log10 of the spore loads. The model included the log10 of spores as the fixed effect and, as random effects, the intercepts for the DNA extractions batch (1 | de) (n = 3) and qPCR run (1 | qpcr) (n = 2). Visual inspection of the model showed no deviation from linearity, homogeneity of variance, or normality. The estimates of the lmer were used to determine the qPCR efficiency according to Equation 1.

$$E_{st} = (10^{-\frac{1}{n}} - 1)\ x\ 100 \qquad \text{Equation 1}$$

E_{st} denotes the qPCR efficiency according to the standard-curve analysis and n the lmer estimate for the log10 of spores in spore traps [22,26]. The samples corresponding to the spore traps with $1x10^2$ spores/ml were excluded from the analysis as these traps were below the linear dynamic range of the qPCR [26]. For the amplification curve analysis, a linear model was used to correlate the log10 of the qPCR relative fluorescence units (RFU) with the cycles in the exponential region of the amplification curves. Then, we used the model estimates, Equation 2 and Equation 3, to determine the qPCR efficiency for each amplification curve (E_{am}).

Preprints (www.preprints.org) | NOT PEER-REVIEWED | Posted: 19 September 2022 doi:10.20944/preprints202209.0267.v1

$$log_{10}(RFU) = log_{10}(RFU_0) + log_{10}(E_{am})\ x\ C \qquad \text{Equation 2}$$

$$E_{am} = 10^{m} \qquad \text{Equation 3}$$

In Equation 2, RFU_0 is the RFU at cycle 0, C is the number of cycles, and in Equation 3, m is the slope estimate for the linear model [25]. the E_{am} and E_{st} were used to estimate the standard curve actual dilution and systematic pipetting with Equations 4 and 5 [25].

$$E_{st} = E_{am.st}^{\frac{log_{10}(D)}{log_{10}(A)}} \qquad \text{Equation 4}$$

$$A = Dx(1 + P) \qquad \text{Equation 5}$$

$E_{am,st}$ is the mean of the E_{am}, and D, A, and P are the desired dilution, the actual dilution, and the systematic pipetting error, respectively. Differences in the E_{am} between samples were evaluated using an anova analysis. These analyses used the function *lmer* of the R library *lme4* (version 1.1-26) [27], the *tab_model* function of the R library *sjPlot* (version2.8.9) [28], and the *aov* and *lm* functions of the R library *stat* (version 4.0.4) [24]. The results of the standard curve analysis were visualized using the R library *ggplot2* (version 3.3.3) [23].

2.6. Spore evaluation in the field

The spore-trap devices were evaluated in a commercial cocoa farm in Palestina, Caldas, Colombia (5°4'14.7 "N 75°41'4.4 "O) in October 2021. Specifically, three spore-trap devices (devices 1 to 3) were placed 50 meters apart and allowed them to collect spores and weather data for 14 h, between 6:00 p.m. and 8:00 a.m. The blades' speed was set at 60 rpm, and the climatic variables (i.e., temperature and relative humidity) were collected at one-minute intervals. The spore traps with the environmental samples were gathered and placed separately in 50 ml falcons. Then, the samples were sent to the EAFIT University facilities for their evaluation. The DNA was extracted as explained above (refer to DNA extractions from fungi and spore tramp) and used to estimate the *M. roreri* spore load in the spore traps with qPCR. As an important remark, this study did not intend to evaluate the association between environmental *M. roreri* spore loads and climatic variables, as further evaluations will address this correlation. However, the weather data was extracted from the spore-trap device and visualized to assess the sensors' functionality.

The Ct and E_{am} of the spore traps were estimated and used to calculate the *M. roreri* spore load in the spore traps. Two methods for these calculations were used; first method was the absolute quantification with the dilution of the standard method (standard-curve quantification), and the other was the absolute quantification without dilution of the standard with the E_{am} correction method (single-standard quantification) [25]. For the former, we used the estimates of the lmer correlating the Ct values with the log10 of spores in spore traps (refer to qPCR characterization and validation). Equation 6 was used with $2x10^6$ spores as standard for the latter. In Equation 6, N_0 denotes the *M. roreri* spores load in spore traps, and the *fs* and *st* subscripts refer to field samples and standards, respectively.

$$N_{0,fs} = N_{0,st}x(\frac{E_{am,st}^{CT_{st}}}{E_{am,fs}^{CT_{fs}}}) \qquad \text{Equation 6.}$$

An anova analysis was implemented to assess differences in spore estimates between methods and spore-trap devices after the log10 transformation of the data to satisfy the

 doi:10.20944/preprints202209.0267.v1

anova assumptions. This analysis used the *aov* and *lm* functions of the R library *stat* (version 4.0.4) [24].

3. Results

3.1 Primers' specificity

The initial step for developing a technique to assess the environmental *M. roreri* spore load was to design a pair of *M. roreri*-specific primers. We decided to focus on the ITS region of the ribosomal DNA of *M. roreri,* as sequences for this region are the most abundant for *M. roreri and closely related fungi*. Sequence alignment of fungal ITS revealed potential primer-binding sites that would distinguish between *M. roreri* and other fungi. Therefore, a pair of primers (Mr_ITSF and Mr_ITSR) were designed targeting these regions. In the binding sites of these primers, the alignment of the *M. roreri* and other fungi ITS sequences showed several single-nucleotide polymorphisms (SNPs). However, SNPs were fewer for the *M. roreri* and *M. perniciosa* ITS and were located towards the primers' 5'-end (Figure S2). Thus, it was likely that the Mr_ITSF and Mr_ITSR primers would amplify the ITS regions of both *Moniliophthora* species. Despite this limitation, we decided to continue with this primer pair as witches' broom incidence is low in Colombia and is not limiting [4]. Also, this primer pair was the most suitable for qPCR.

Mr_ITSF and Mr_ITSR primers distinguished *Moniliophthora* spp. from other fungi in the conventional PCR assay. While the generic primers (ITS1 and ITS4) amplified nearly 550 bp ITS segments in all evaluated fungi (Figure 2, upper panel), the Mr_ITSF and Mr_ITSR primers amplified about 320 bp ITS fragments only from *M. roreri* strains MR1 and MR2 and *M. perniciosa* (Figure 2, lanes 11-20).

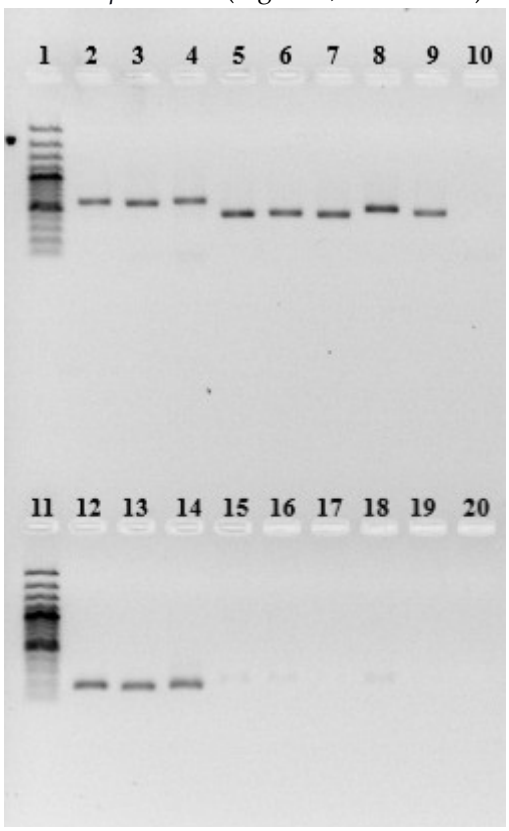

Figure 2. Agarose gel showing the PCR products for the ITS fragments of *Moniliophthora roreri* and other fungi amplified with the ITS1 and ITSR4 (Lanes: 1-10) and the Mr_ITSF and Mr_ITSR primers (Lanes: 11-20). Lanes 1 and 11: 100 bp ladder. Lanes 2 and 12: *M. roreri* strain MR1. Lanes 3 and 13: *M. roreri* strain MR2. Lanes 4 and 14: *M. perniciosa*

 doi:10.20944/preprints202209.0267.v1

basidiocarp. Lanes 5 and 15: *Diaporthe* sp. EAFIT-F0056. Lanes 6 and 16: *Alternaria* sp. EAFIT-F0059. Lanes 7 and 17: *Colletotrichum* sp. EAFIT-F0066. Lanes 8 and 18: *Pleurotus* sp. Lanes 9 and 19: *Ganoderma* sp. Lanes 10 and 20: Non-template control.

3.2 DNA extraction from spore tramps

Spore traps were inoculated with *M. roreri* spore loads between $2x10^2$ and $2x10^6$ to assess whether it could extract DNA from spores in spore traps. The amount of DNA extracted from $2x10^6$ non-trapped spores was close to 6 µg, almost x10 higher than that of spore traps with $2x10^6$ spores (800 ng). For the other spore trapped, only was possible to measure the extracted DNA for those with $2x10^5$ spores (200 ng) since the amount in the others was too low to be quantified by NanoDrop. *These results showed* that our protocol was successful in extracting DNA from *M. roreri* spore in spore traps. However, the extraction was less efficient for trapped than for non-traped spores.

The expected 550 bp-ITS fragments were amplified using primers ITS1 and ITS4 and the DNA extracted from spore traps with 2×10^4 spores and higher as the template (Figure 3). However, no amplicon from DNA of spore traps with 2×10^3 spores or less were detected by PCR, probably due to the low amounts of DNA extracted. These findings indicate that the quantity and quality of the DNA extracted were sufficient to detect *M. roreri* spores from spore traps with spore loads of at least 2×10^4 with PCR. However, a more sensitive technique such as qPCR would be necessary to detect and quantify lower spore loads.

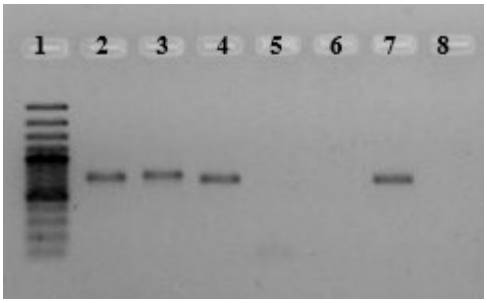

Figure 3. Agarose gel showing the ITS PCR products for *Moniliophthora roreri* spores captured by spore traps. DNA was extracted from spore traps inoculated with x10n spore loads between 2×10^2 and 2×10^6 and used to amplify fragments of the ITS sequence segments with ITS1 and ITS4 primers. Lane 1: 100 bp ladder. Lane 2-6: Spore traps with × 10n spore loads between 2×10^2 and 2×10^6. Lane 7: *M. roreri* strain MR1. Line 8: Non-template control.

3.3. Specificity of the qPCR

All *Moniliophthora* samples (mycelia, spores in spore traps, and non-trapped spores of *M. roreri* and *M. perniciosa* basidiocarp) had Ct values between 15 cycles and 29 cycles. These Ct were lower than those of the non-*Moniliophthora* strains and non-template controls (> 30 cycles, p-value < 0.001) despite using comparable or higher DNA amounts in the qPCR reactions (Table 1). These lower Ct agree with the agarose gel showing a 320 bp-amplicon only for *Moniliophthora* samples (Figure S3). These results show the specificity of the qPCR reactions for *Moniliophthora* spp., at least among the evaluated fungi. Comparing the *Moniliophthora* samples, the Cts of *M. roreri* strain MR1 were nearly three-cycle higher than those of *M. perniciosa* basidiocarp in qPCR reactions using comparable

Preprints (www.preprints.org) | NOT PEER-REVIEWED | Posted: 19 September 2022 doi:10.20944/preprints202209.0267.v1

amounts of DNA (~ 40 ng) (Table 1). This result suggests an extent of specificity for the Mr_ITSF and Mr_ITSR primers towards *M. roreri*. However, this specificity is not enough to differentiate between the two species that belong.

Table 1. qPCR DNA loadings, replicates, and estimates for *Moniliophthora roreri*, other fungi, and cacao field samples.

Samples	qPCR				Spore loads (x 10000)	
	Ct[a] (mean ± SD)	n[b]	DNA (ng)	Ef_{am}[c] (mean ± SD)	St. curve	Am. curve
Moniliophthora roreri						
Spore in spore traps						
2×10^6	16.1 ± 1.4	12	45.8 - 50.6	1.88 ± 0.09	-	-
2×10^5	21.5 ± 1.8	10	11.1-12.3	1.90 ± 0.06	-	-
2×10^4	26.8 ± 2.6	11	ND[e]	1.87 ± 0.08	-	-
2×10^3	28.9 ± 1.1	12	ND	1.86 ± 0.04	-	-
2×10^2	28.7 ± 1.6	12	ND	1.88 ± 0.08	-	-
Non-traped spores						
2×10^6	15. 0 ± 1.6	12	365.4-495.3	1.93 ± 0.05	-	-
Strain MR1	20.0 ± 0.5	2	37.7	1.85 ± 0.07	-	-
Strain MR2	-	-	-	-	-	-
Moniliophthora perniciosa						
Basidiocarp	23.1 ± 0.5	2	40.0	1.82 ± 0.02	-	-
non-*Moniliophthora* strains						
Ganoderma sp.	33.8 ± 0.2	2	39.3	1.86 ± 0.01	-	-
Pleurotus sp.	32.8 ± 0.4	2	35.7	1.87 ± 0.07	-	-
Diaporthe sp. EAFIT-F056	30.3 ± 0.9	2	27.0	1.94 ± 0.02	-	-
Alternaria sp. EAFIT-F059	30.9 ± 1.3	2	10.2	1.89 ± 0.05	-	-
Colletotrichum sp. EAFIT-F066	32.1 ± 0.7	2	5.8	2.02 ± 0.04	-	-
Field samples						

Preprints (www.preprints.org) | NOT PEER-REVIEWED | Posted: 19 September 2022 doi:10.20944/preprints202209.0267.v1

	Device 1	23.5 ± 0.1	2	ND	1.89 ± 0.00	4.60 ± 0.34	1.80 ± 0.16
	Device 2	25.2 ± 0.1	2	ND	1.80 ± 0.01	1.90 ± 0.12	2.10 ± 0.14
	Device 3	28.0 ± 0.1	2	ND	1.88 ± 0.02	0.44 ± 0.02	0.11 ± 0.17

[a] Ct, qPCR threshold cycle

[b] n, number of replicates

[c] Ef_{am}, qPCR efficiency according to the amplification-curve analysis.

[d] Number of spores estimates for the quantification with the standard-curve (St. curve) and the amplification-curve (Am. curve) quantification

[e] ND, not detected.

3.3. qPCR efficiency, variability, and limit of detection for the quantification and detection of M. roreri *spores in spore traps*

The detection probability of *M. roreri* spores in spore traps formed a sigmoid curve against the log10 of spores, with this probability being 1 for *M. roreri* spores in spore traps with spore loads over 2 x 10^5 and closer to 0 as the spore load dropped (Figure 4 A, Table S2). The qPCR's 90 % and 95 % detection limits were 1.5 x 10^4 and 3.9 x 10^4 spores, respectively (Figure 4 A). The technique detected lower spore loads, but the risk of a false negative increased for small spore loads. *M. roreri* spores were detected in 80 % and 50 % of spore traps with 2 x 10^4 and 2 x 10^3 spores, respectively. Contrastingly, spores of *M. roreri* from spore traps inoculated with 2x10^2 spores were detected only in 17 %.

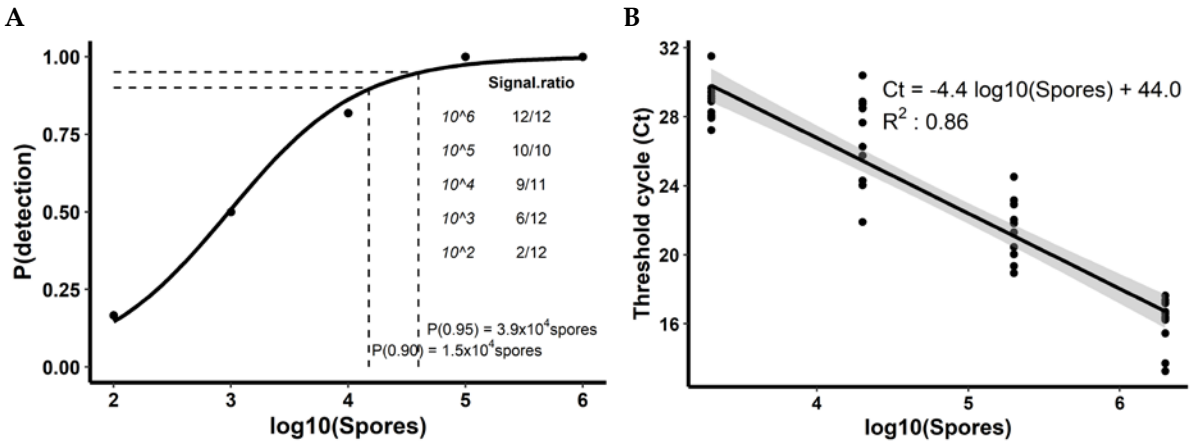

Figure 4. DNA extraction and quantification of *Moniliophthora roreri* spores in spore traps. DNA was extracted from spore traps inoculated with x10n spores between 2 x 10^2 and 2 x 10^6 and used in qPCR reactions with Mr_ITSF and Mr_ITSR primers. Six spore traps per log 10 of spore were evaluated in two separated qPCR, each containing two technical replicates per sample. Non-template controls (n = 6) and DNA of *M. roreri* strain MR1 (n = 2) were included in every qPCR as controls. In A, shows the correlation between the detection probability (i.e., return a positive qPCR) and the logarithm with base 10 (log10) of *M. roreri* spores in spore traps. The points represent the probability of spore traps returning a positive qPCR, defined as a qPCR reaction with a Ct five cycles below the non-template controls. The solid line represents the prediction of the general linearize model (GLM) with the logit function and the binomial family error. The dashed lines represent the qPCR's 95 % and 90 % detection limits. The statistics of the GLM are shown in Table S2. B) shows the correlation between

 doi:10.20944/preprints202209.0267.v1

the qPCR threshold cycle (Ct) and log10 of *M. roreri* spores in spore traps. The points (n = 12 per log10 of spore) represent the average between both technical replicates. The line and the gray area represent the prediction and standard error of the linear mixed-effects model (lmer), respectively. The statistics of the lmer are shown in Table S3.

The qPCR's linearity range was between 2 x 10^3 and 2 x 10^6 spores, as indicated by the correlation between Ct values and the log10 of *M. roreri* spores in spore traps (Figure 4 B; Table S3). We excluded the spore traps with 2x10^2 spores from this analysis as this spore load had a low detection probability (close to 17 %) (Figure 4 A), and its inclusion lowered the fitting of the lmer (R^2: 0.79 vs. 0.86) (Figure 4 A and Figure S4). In the linearity range, the Ct values lowered around 4.3 cycles for each x10 increase in the spore load (Figure 4 B, Table S3), indicating a qPCR efficiency (E_{st}) of 1.38 (68.8 %). This qPCR efficiency was lower than those estimated using the amplification curves (E_{am}) (Table 1). The E_{am} for the spore traps with spore loads between 2 x 10^3 and 2 x 10^6 was 1.87 on average (SD: 0.09, n: 45) and did not vary between samples (*p-value*: 0.53, according to the anova test). The difference between E_{st} and E_{am} represents a systematic pipetting dilution error of 94% and an actual dilution of x 1/19.4 instead of x 1/10, which was the intended dilution for the standard curve.

The elevated systematic pipetting dilution error agrees with the high variability of the Ct values found between spore trap replicates, showing coefficients of variance (SD/mean) between 3.2 % and 10.9 % (Table 1). Despite the variability, the lmer fitted the data with a 0.86 marginal R^2 and a 0.89 conditional R^2 (Figure 3 C, Table S3), showing that changes in the log10 of spores explained most of the Ct values variability. The DNA extraction batch and the qPCR run explained part of the remaining variability not explained by the log10 of spores, each explaining the 17.5 % and 3.1 % of the Ct variance, respectively (Table S3). These percentages of explained variance show that samples processed in different DNA extraction batches had an additional source of variation that should be considered in the field evaluations. In contrast, the qPCR run in which the DNA was analyzed was less relevant.

3.4. Detection of M. roreri spores in commercial fields of cacao

The above shows that we can detect nearly 2 x 10^4 *M. roreri* spores using spore traps device and qPCR. We wondered whether we could use this strategy to detect and quantify the environmental *M. roreri spore* load in a commercial cacao farm. *M. roreri* spores were detected in all the field samples, with all spore traps with field samples having Ct values between 23 and 28 cycles. These Ct values were below those of non-template controls and non-*Moniliophthora* fungal strains and were comparable to those of spore traps with 2x10^4 *M. roreri* spores (Table 1). A single 320-bp amplicon in the agarose gel validated the Ct values in these field samples (Table 1, Figure S3). The quantification method (standard-curve and single-estimate quantification) and spore-trap device affected the *M. roreri* spore load estimates (Table S4). However, the effect was more pronounced for the spore-trap device (Table S4). The standard-curve quantification resulted in estimates higher (between 4.4 x 10^3 and 4.6 x 10^4 spores per spore trap) than those of the single-standard quantification (between 1.1 x 10^3 and 2.1 x 10^4 spores per spore trap). However, these estimates remained in the same order of magnitude within devices (Table 1).

Comparing spore-trap devices, the estimates for the device with the highest *M. roreri* spore load estimates (device 1) were over one order of magnitude (x 10.5 and x 19.9 for the standard-curve and single-estimate quantification, respectively) than those of the device with the least number of *M. roreri* spores (device 3) (Table 1). It is unknown whether these differences have biological relevance since the spore-trap devices were placed only 50 mt apart. Despite these between-devices differences, all the estimates were above the qPCR's 50 % detection limit technique (2.0 x 10^3 spores per spore trap) regardless of the quantification method (Table 1, Figure 4 A). Two devices (devices 1 and 2) had estimates above the qPCR's 90 % detection limit (1.1 x 10^5 spores per spore trap). Besides trapping the spores, the spore-trap devices recorded climatic variables at one-minute intervals. The

 doi:10.20944/preprints202209.0267.v1

data was downloaded into a computer to be further analyzed (Table S5). This study did not aim to correlate the *M. roreri* spore loads with the climatic variables, as further work will address this correlation. However, we wanted to assess the functionality of the spore-trap devices.

4. Discussion

Coupling spore traps device with qPCR technique is a reliable method for detecting and quantifying spores of fungal plant pathogens in the field [16–19] and could be useful for assessing the *M. roreri* spore loads in cacao plantations. Therefore, we developed in parallel a spore-trap device that carries spore traps while recording climatic variables and standardized a qPCR protocol to detect and quantify the *M. roreri* spore loads in the spore traps. This method was evaluated with spore traps inoculated with a known *M. roreri* spore loads under condition of laboratory and evaluated under cacao-field environmental. According to our estimations, this method can detect above 2000 spores in one load of field samples.

Air-born spores of several fungi, including plant pathogenic and non-pathogenic fungi, populate the crops' air. Molecular biology techniques such as PCR and qPCR can help in distinguishing pathogenic populations from other environmental fungi using specific primers [16,22,29]. The primers here reported were successful in distinguishing *M. roreri* from fungi in a different genus. However, they failed to distinguish *M. roreri* from its close relative, *M. perniciosa* [4]. The lack of specificity between the *Moniliophthora* species is inconvenient since *M. perniciosa* is also a cacao pathogen responsible for the Witches' broom. Therefore, *M. perniciosa* spores in the environment can result in an overestimated *M. roreri* spore load. In Colombia, Witches' broom (WBD) is a disease secondary to FPR, as its derived losses are lower [4]. However, in other countries such as Brazil, WBD is more relevant than FPR, the latter having recently announced its arrival in the producing country [3]. Compared with *M. roreri, M. perniciosa* is easier to control, less pathogenic, and less prevalent, at least in Colombia [4,30]. Therefore, it would be expected to have a minimal impact of *M. perniciosa spores in the M. roreri* spore load estimates. However, no work has evaluated the *M. perniciosa* spore load in Colombian cacao fields, and its effect on the *M. roreri* spore load estimations might be relevant.

Besides selective, a method for assessing spore loads of plant pathogenic fungi must be sensitive since spore loads are low in the field [22]. The method here described can detect 1.5×10^4 spores of *M. roreri* with 90 % of confidence and 3.9×10^4 spores *M. roreri* with 95 % of confidence. These detection limits were higher than those reported in other studies, meaning our technique is less sensitive [31]. However, comparing our detection limits with other evaluations might not be appropriate for several reasons. First, most of these evaluations used DNA instead of spores suspensions to estimate their detection limits [29,31]. Therefore, the detection limits do not represent the complexity of the biological sample. They ignore the difficulties of extracting DNA from fungal spores, especially when trapped in the spore trap [22,25]. This work showed that the efficiency of DNA extraction of *M. roreri* spores collected from spore traps was nearly ten times lower than that of non-traped spores, which does not consider the efficiency penalty of extracting DNA from fungal spores. Second, these evaluations also ignore the effect of the sample context and components on the qPCR efficiencies. We did not evaluate this effect, but it is not neglectable [25,32]. Finally, these evaluations do not attach a confidence level to their detection limits, which can be miss leading [29,31].

The amount of DNA target estimated by qPCR can be a relative or absolute value, depending on the estimation method [25]. Standard-curve quantification is the most common method for estimating absolute values [22,25,26]. This method correlates the Ct values of serial dilutions of the target with the target amount in the dilutions. Then, it uses this correlation to estimate the target amount in an unknown sample [22]. Most evaluations assessing airborne spores of plant pathogenic fungi used this method [16,19,29,31,33]. However, pipetting and systematic dilution errors in the standard curve

Preprints (www.preprints.org) | NOT PEER-REVIEWED | Posted: 19 September 2022 doi:10.20944/preprints202209.0267.v1

preparation can diminish the estimations' reliability [25]. In this work, the standard curves varied between qPCR runs and found that these standard curves were more diluted than intended. These variability and dilution errors probably led to inaccuracies in the estimates of the *M. roreri* spore loads in spore traps [25,32]. An alternative to standard-curve quantification is single-standard quantification [25]. Both methods were compared since the single-standard quantification is a simpler method and the *M. roreri* spore estimates varied between methods, but the differences were small. Therefore, we recommend using the single-standard quantification method to assess *M. roreri* spore loads in cacao plantations.

In terms of the field evaluations, spore loads were estimated between 1.0×10^3 and 4.0×10^4. These estimates were using the method for limit detection above 90 %, indicating that the method was sensitive enough to estimate the *M. roreri* spore load in the cacao farm. The spore-trap devices sampled nearly four liters of air (4.08 L) per min, considering its geometry and rotor speed. Therefore, the estimated spore loads translate to 2.5×10^2 and 1.0×10^4 *M. roreri* spores per m^3 of air. These values agree with values reported by similar evaluations in other systems (i.e., between 1.0 and 1.0×10^5 spores or DNA copies per m^3 of air) [18,19,34]. To our knowledge, no comparable analyses have evaluated the *M. roreri* spore load in cacao fields. However, an older study using passive spore traps and microscopy detected between 30 and 144 *M. roreri* spores per cm^2 of spore trap in an 8-h evaluation period [5]. Here were detected between 61 and 246 *M. roreri* spores per cm^2 of spore trap, which are comparable values despite the differences in methods and sampling period.

Even though we only evaluated the method for assessing the *M. roreri* spore load once in the field, we consider that the method here developed (coupling device and qPCR) has great potential for estimating natural pathogen populations. Therefore, more evaluations must validate the results obtained, these new evaluations must include multiple cacao farms and consider the effect of *M. perniciosa* spores into spore load. Future studies can use this method to characterize the dynamics of *M. roreri* spore loads in different cacao growing regions and assess the weather's effect on the epidemiology of the Frosty pod rod.

Supplementary material

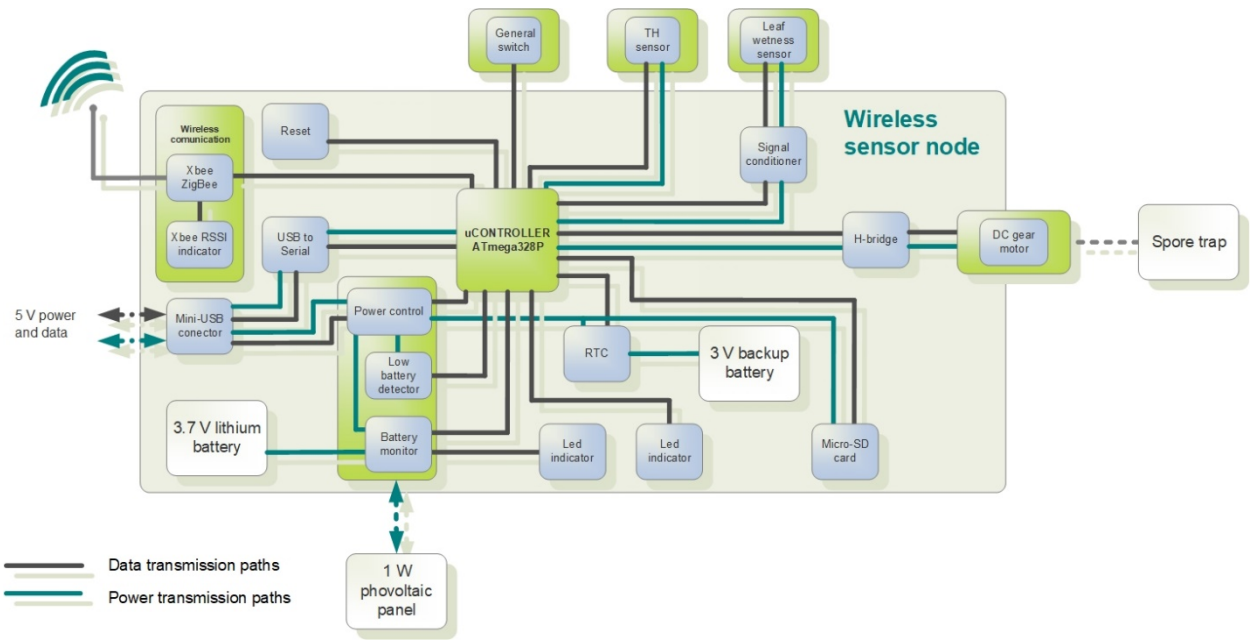

Preprints (www.preprints.org) | NOT PEER-REVIEWED | Posted: 19 September 2022 doi:10.20944/preprints202209.0267.v1

Figure S1. Block diagram showing the main components of the spore-trap devices.

```
                <--to ITS1
MR_Reference    GGGCATGTGCTCGCCGACTTTCAATCTTCATCCACCTGTGAACCTTTTGTAGTGGATTCT
MR1             GGGCATGTGCTCGCCGACTTTCAATCTTCATCCACCTGTGAACCTTTTGTAGTGGATTCT
MR2             GGGCATGTGCTCGCCGACTTTCAATCTTCATCCACCTGTGAACCTTTTGTAGTGGATTCT
M.perniciosa_IT GGGCATGTGCTCGCCGACTTTCAATATTCATCCACCTGTGAACCTTTTGTAGCAGATTCT


MR_Reference    GGAAC-GGGAGGCGCTTGCGTTT-TCTCAGTACGGAGTCTCAC---TATGTTTTAACACA
MR1             GGAACGGGGAGGCGCTTGCGTTT-TCTCAGTACGGAGTCTCAC---TATGTTTTAACACA
MR2             GGAACGGGGAGGCGCTTGCCTTT-TCTCAGTACGGAGTCTCAC---TATGTTTTAACACA
M.perniciosa_IT GGAATAGGGAGGCGCTTGCGTTTCTCTTAGTACGGAGTCTACTATGTTTGTTTTTTAACA
                           Mr-ITSF >>>>>>>>>>>>>>>>>>>>>>

MR_Reference    CACTTAATGTATGTTTAGAATGTGTATTTTATTGGGACTTAATTGACCCTTTAAAAACTA
MR1             CACTTAATGTATGTTTAGAATGTGTATTTTATTGGGACTTAATTGACCCTTTAAAAACTA
MR2             CACTTAATGTATGTTTAGAATGTGTATTTTATTGGGACTTAATTGACCCTTTAAAAACTA
M.perniciosa_IT CACTTAATGTATGTTTAGAA--TGTATTTTATTGGGACTTAATTGACCCTTT-AAAACTA


MR_Reference    TACAACTTTCAGCAACGGATCTCTTGGCTCTCGCATCGATGAAGAACGCAGCGAAATGCG
MR1             TACAACTTTCAGCAACGGATCTCTTGGCTCTCGCATCGATGAAGAACGCAGCGAAATGCG
MR2             TACAACTTTCAGCGACGGATCTCTTGGCTCTCGCATCGATGAAGAACGCAGCGAAATGCG
M.perniciosa_IT TACAACTTTCAGCAACGGATCTCTTGGCTCTCGCATCGATGAAGAACGCAGCGAAATGCG


MR_Reference    ATAAGTAATGTGAATTGCAGAATTCAGTGAATCATCGAATCTTTGAACGCACCTTGCGCC
MR1             ATAAGTAATGTGAATTGCAGAATTCAGTGAATCATCGAATCTTTGAACGCACCTTGCGCC
MR2             ATAAGTAATGTGAATTGCAGAATTCAGTGAATCATCGAATCTTTGAACGCACCTTGCGCC
M.perniciosa_IT ATAAGTAATGTGAATTGCAGAATTCAGTGAATCATCGAATCTTTGAACGCACCTTGCGCC


MR_Reference    TCTTGGTATTCCGAGAGGCATGCCTGTTTGAGTGTCATTAAATTCTCAACCTCAAA-AAG
MR1             TCTTGGTATTCCGAGAGGCATGCCTGTTTGAGTGTCATTAAATTCTCAACCTCAAAAAAG
MR2             TCTCGGGATTCCGAGAGAGATGCCTGTTTGAGTGTCATTAAATTCTCAACCTCAAAAAAG
M.perniciosa_IT TCTTGGTATTCCGAGAGGCATGCCTGTTTGAGTGTCATTAAATTATCAACCTTGAATGAC


MR_Reference    CTTTTTCGGCTTTGTTTGAGGATTGGATGTGAGGGTTGCTGGCTTTTTGAATAAAGAGTC
MR1             CTTTTTCGGCTTTGTTTGAGGATTGGATGTGAGGGTTGCTGGC-TTTTGAATAAAGAGAC
MR2             CTTTTTCGGCTTTGTTTGAGGATTGGATGCGAGGGTCGCTGGC-TTTTGAATAAAGAGAC
M.perniciosa_IT TT--------GTCATTTCAGGATTGGATGTGAGGGCTGCCGGC--TTTGAAC-AAGAGTC


MR_Reference    GGCTCCCTTGAAATGCATTAGTGGAAACCGGT-TGGTAGACCACATTGGTGT
MR1             GGCTCCCTTGAAATGCATTAGTGGAAACCGGT-TGGTAGACCACATTGGTGT
MR2             CGCTCCCTTGAAATGGATTAGTGGTTACCGGG-TGGTAGACCACATTGGTGT
M.perniciosa_IT GGCTCTCTTGAAATGCATTAGTGGAAACCGCTATAGTGGACCACATTGGTGT
                                  <<<<<<<<<<<<<<<<<<<< Mr-ITSR|to ITS4 -->
```

Preprints (www.preprints.org) | NOT PEER-REVIEWED | Posted: 19 September 2022 doi:10.20944/preprints202209.0267.v1

Figure S2. Binding sites of the Mr_ITSF and Mr_ITSR primers for the ITS aligned sequences *of the Moniliophthora roreri* strains MR1 (OM056945), MR2 (OM056946), and MCA2954 (Genbank DQ222927), and *Moniliophthora perniciosa* basidiocarp (OM056947). >>> and <<< represent the primers' binding sites.

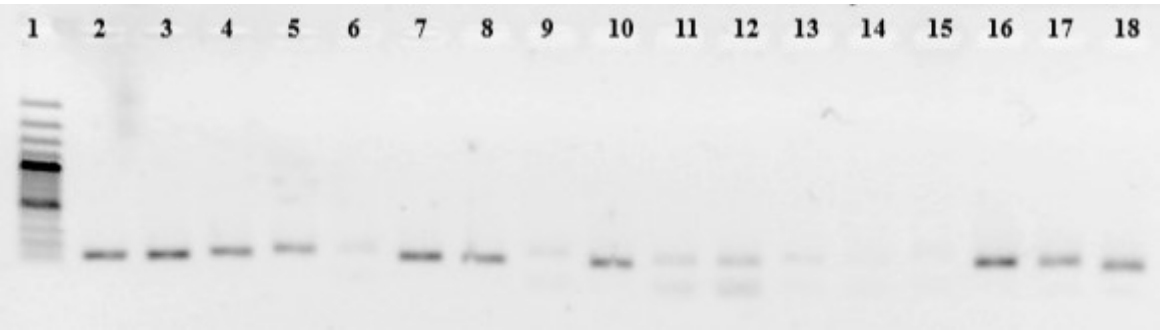

Figure S3. Agarose gel showing the qPCR products of the ITS fragments of *Moniliophthora roreri* and other fungi amplified with the Mr_ITSF and Mr_ITSR primers. Lane 1: 100 bp ladder. Lane 2-6: spore traps with x 10n *M. roreri* spore loads between 2 x 10^6 and 2 x 10^2. Lane 7: 2x10^6 non-trapped *M. roreri* spores. Lane 8: *M. roreri* strain MR1. Lane 9: Non-template control. Lane 10: *M. perniciosa* basidiocarp. Lane 11: *Diaporthe* sp. EAFIT-F0056. Lane 12: *Alternaria* sp. EAFIT-F0059. Lane 13: *Colletotrichum* sp. EAFIT-F0066. Lane 14: *Pleurotus* sp. Lane 15: *Ganoderma* sp. Lane 16-18: spore traps with the field samples collected in a cacao farm in Palestina, Caldas, Colombia.

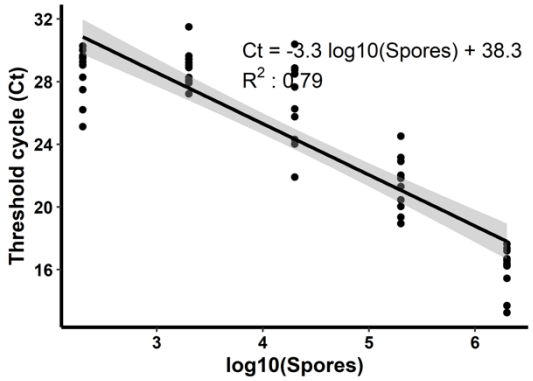

Figure S4. Correlation between the qPCR threshold cycle (Ct) and the logarithm with base 10 (log10) of *Moniliophthora roreri* spores in spore traps. DNA was extracted from spore traps inoculated with x10n spores between 2 x 10^2 and 2 x 10^6 and used in qPCR reactions with Mr_ITSF and Mr_ITSR primers. Six spore traps per log 10 of spore were evaluated in two separated qPCR, each containing two technical replicates per sample. Non-template controls (n = 6) and DNA of

 doi:10.20944/preprints202209.0267.v1

M. roreri strain MR1 (n = 2) were included in every qPCR as controls. The line and the gray area represent the prediction and standard error of the linear mixed-effects model (lmer), respectively.

Table S1. Fungal strains, primers, and fungal ITS sequences used in this study.

Strain	Molecular identity			Origin
	Closest sequence[a]	GB AN[b]	HI[c]	
MR1	*Moniliophthora roreri*	MH861051	100	Isolated during the study
MR2	*Moniliophthora roreri*	KU674835	100	Isolated during the study
ND	*Pleurotus* sp.	MK673812	100	Culture collection Universidad EAFIT
ND	*Ganoderma* sp.	unpublished	ND	Culture collection Universidad EAFIT
EAFIT-F0056	*Diaporthe phaseolorum*	MN997107	99.8	Culture collection Universidad EAFIT
EAFIT-F0059	*Alternaria argyroxiphii*	NR136074	100	Culture collection Universidad EAFIT
EAFIT-F0066		MZ066745	99.1	Culture collection Universidad EAFIT
N.A.	*Moniliophthora perniciosa*	MH861049	100	Basidiocarp collected during the study

Primer	Sequence	Target	Reference
ITS1	TCCGTAGGTGAACCTGCGG	Fungal ITS	(Raja et al. 2017)
ITS4	TCCTCCGCTTATTGATATGC	Fungal ITS	(Raja et al. 2017)
Mr-ITSF	ATTGGGACTTAATTGACCCTTT	*M. roreri* ITS	This study
Mr-ITSR	TCTACCAACCGGTTTCCACT	*M. roreri* ITS	This study

ITS GB AN[b]	Fungal specie	Fungal strain	Sequence size (bp)
OM056945[d]	***Moniliophthora roreri***	**MR1**	**665**

 doi:10.20944/preprints202209.0267.v1

OM056946	***Moniliophthora roreri***	**MR2**	**683**
JX515287	*Moniliophthora roreri*	B1b	687
JX515288	*Moniliophthora roreri*	B2a	684
JX315285	*Moniliophthora roreri*	E16	680
JX315273	*Moniliophthora roreri*	SPCL	680
MH861051	*Moniliophthora roreri*	CBS 202.77	687
KU674835	*Moniliophthora roreri*	CBS138635	687
JX315282	*Moniliophthora roreri*	Co12	680
JX515290	*Moniliophthora roreri*	B3	687
JX515291	*Moniliophthora roreri*	B4	687
AY230254	*Moniliophthora roreri*	ND[e]	687
OM056947	***Moniliophthora perniciosa***	**ND**	**665**
MK785162	*Moniliophthora perniciosa*	RWB1268	704
MK785163	*Moniliophthora perniciosa*	DIS70	749
MK785161	*Moniliophthora perniciosa*	RWB1267	739
MK785160	*Moniliophthora perniciosa*	RWB1205	688
MK785159	*Moniliophthora perniciosa*	RWB1065	488
MK785158	*Moniliophthora perniciosa*	COAD2616	751
MK785157	*Moniliophthora perniciosa*	COAD2615	746
MK785142	*Moniliophthora perniciosa*	COAS2600	735
MK785141	*Moniliophthora perniciosa*	COAS2599	734
MK785140	*Moniliophthora perniciosa*	COAD2598	745
MK785139	*Moniliophthora perniciosa*	COAD540	712
KY081771	*Moniliophthora perniciosa*	WMA14(B)	657
KY081770	*Moniliophthora perniciosa*	WMA5	657
KY081769	*Moniliophthora perniciosa*	SCFT	660
KY081768	*Moniliophthora perniciosa*	LJ8	672
EU514248	*Pseudocercospora fijiensis*	CBS 120258	525

 doi:10.20944/preprints202209.0267.v1

AY616686	*Entonaema liquescens*	agtS279	477
KF225610	*Cytospora atrocirrhata*	HMBF156	540
JQ005152	*Colletotrichum gloeosporioides*	CBS 112999	536
JQ005776	*Colletotrichum acutatum*	CBS 112996	544
KJ909769	*Bipolaris maydis*	CBS136.29	677
AM749934	*Daldinia caldariorum*	JPP 26211	484
FJ889444	*Diaporthe alleghaniensis*	CBS 495.72	543
AF388914	*Neurospora crassa*	FGSC 987	561
KX986055	*Nigrospora oryzae*	LC6760	524
FJ889450	*Phomopsis cotoneastri*	CBS 439.82	545

[a] Fungal strain with the highest ITS sequence similarity according to BLAST.

[b] GeneBank accession number.

[c] Highest Identity, values between 0 and 100 %. ND not defined.

[d]Bold sequences are the sequences submitted to the GeneBank during this study

[e]ND, no defined

Table S2. Estimates for the general linearize model (glm) with the logit function and the binomial family error for the detection probability of the logarithm with base 10 (log10) of *Moniliophthora roreri* spores in spore traps.

model: glm (Probability ~ log10(spores), family = binomial)				
Fixed effects				
	Odds Ratios	**St. Error**	**CI**	**p-value**
Intercept	0.0	0	0.0 - 0.1	<0.001
log10(spores)	6	2.9	2.7 - 18.8	<0.001
Observations				5
Null deviance				33.2

 doi:10.20944/preprints202209.0267.v1

Residual deviance				0.83
AIC				12.6
Null model: glm (Probability ~ 1, family = binomial)				
Fixed effects				
	Odds Ratios	**St. Error**	**CI**	**p-value**
Intercept	2.2	--	0.0 - 0.1	0.007
Observations				5
Null deviance				33.2
Residual deviance				33.2
AIC				43.1

Table S3. Estimates for the linear mixed model (lmer) correlating the qPCR threshold cycle (Ct) and the logarithm with base 10 (log10) of *Moniliophthora roreri* spores in spore traps.

model: lmer(Ct ~ log10(spores) + (1|de) + (1|qpcr))				
Fixed effects				
	Estimate	**St. Error**	**CI**	**p-value**
Intercept	44.0	1.3	41.4 - 46.6	<0.001
log10(spores)	-4.4	0.2	-4.9 - -3.9	<0.001
Random effects				
Groups	**name**	**Variance**	**n**	
de	Intercept	0.73	3	
qpcr	Intercept	0.13	2	
Residual		3.3		
Observations				45

 doi:10.20944/preprints202209.0267.v1

Marginal R^2	0.86
Conditional R^2	0.89

[a] de, DNA extraction batch; qpcr; qPCR run.

Table S4. Summary of the anova assessing differences in the logarithm base 10 (log10) of *Moniliophthora roreri* spores estimates between spore trap devices and quantification methods (standard-curve quantification vs. single-estimate quantification) in the field experiment.

model: aov(log10(spores) ~ device *method)					
	Df	**Sum Sq**	**Mean Sq**	**F-value**	**Pr(>F)**
method	1	0.38	0.38	214.4	<0.001
device	2	2.69	1.34	762.8	<0.001
method:device	2	0.14	0.07	38.5	<0.001
Residual	4	0.01	0.01		<0.001

Table S5. Example of the first rows of the .csv file obtained during the field experiment for one of the spore trap devices containing the temperature (ºC), relative humidity (%), date, and time.

23.74,60.94,1/1/0,17:6:16

23.71,60.94,1/1/0,17:6:17

23.71,60.94,1/1/0,17:6:18

23.69,60.95,1/1/0,17:6:19

23.69,60.98,1/1/0,17:6:20

23.69,61.02,1/1/0,17:6:21

23.71,60.98,1/1/0,17:6:22

23.68,60.99,1/1/0,17:6:23

23.66,60.99,1/1/0,17:6:39

23.65,61.00,1/1/0,17:6:40

Funding

This work was supported by EAFIT University (Grant No. 954-000005, *Tecnologías Convergentes de Cacao*), Colombian Ministry of Science, Technology, and Innovation (MINCIENCIAS) through a postdoctoral grant (code 848-2019).

Acknowledgments

The authors are thankful for the financial support of this project from the EAFIT University, *MINCIENCIAS* and the Colombian National Government Scholarship (*Ser Pilo Paga*). Casa Luker Company, for allowing us access to their farms where did the field experiment and for providing us with the cacao samples, as well as to Eng. Juan Pablo Gil for helping us in the field experiment.

Author Contributions

Conceptualization, **Javier C. Álvarez,** and **Sandra Mosquera-López**; Methodology, **Javier C. Álvarez** and **Sandra Mosquera-López**; Formal Analysis, **Diana L. Jiménez-Zapata, and Sandra Mosquera-López**; Investigation, **Diana L. Jiménez-Zapata, Manuela Quiroga-Pérez, Manuela Quiroz-Yepes, Alejandro Marulanda-Tobón, Javier C. Álvarez,** and **Sandra Mosquera-López**; Resources, **Javier C. Álvarez**; Data Curation, **Diana L. Jiménez-Zapata, and Sandra Mosquera-López**; Writing – Original Draft Preparation, **Sandra Mosquera-López**; Writing – Review & Editing, Diana **Jiménez-Zapata, Sandra Mosquera-López, Javier C. Álvarez**; Supervision, **Alejandro Marulanda-Tobón, Javier C. Álvarez,** and **Sandra Mosquera-López**; Project Administration, **Javier C. Álvarez**; Funding Acquisition, **Javier C. Álvarez**"

Data availability statement

The authors declare that the data supporting the findings of this study are available within the article.

Conflicts of interest

The authors declare this research was conducted without any commercial or financial relationships that could be construed as a potential conflict of interest.

References

1. Evans, H.C.; Holmes, K.A.; Phillips, W.; Wilkinson, M.J. What's in a Name: Crinipellis, the Final Resting Place for the Frosty Pod Rot Pathogen of Cocoa? *MYT* **2002**, *16*, doi:10.1017/S0269915X02004093.

2. Leandro-Muñoz, M.E.; Tixier, P.; Germon, A.; Rakotobe, V.; Phillips-Mora, W.; Maximova, S.; Avelino, J. Effects of Microclimatic Variables on the Symptoms and Signs Onset of *Moniliophthora roreri*, Causal Agent of Moniliophthora Pod Rot in Cacao. *PLOS ONE* **2017**, *12*, e0184638, doi:10.1371/journal.pone.0184638.

3. Jiménez, D.L.; Alvarez, J.C.; Mosquera, S. Frosty Pod Rot: A Major Threat to Cacao Plantations on the Move. *Trop. plant pathol.* **2021**, doi:10.1007/s40858-021-00472-y.

4. Jaimes, Y.; Aranzazu, F. *Manejo de las enfermedades del cacao (Theobroma cacao L) en Colombia, con énfasis en monilia (Moniliophthora roreri)*; Corporacion Colombiana de Investigacion Agropecuaria - Corpoica, 2010; ISBN 978-958-740-034-2.

5. Ram, A. Biology, Epidemiology and Control of Moniliasis (*Moniliophthora Roreri*) of Cacao, Imperial College of Science and Technology: Ascot, 1989.

6. Torres de la Cruz, H. Temporal Progress and Integrated Management of Frosty Pod Rot (Moniliophthora Roreri) of Cocoa in Tabasco, Mexico. *J. Plant Pathol.* **2011**, *93*, 31–36.

7. Merchán, V.M. Avances de la investigación de la moniliasis del cacao en Colombia. *El cacaotero Colombiano* **1981**, 26–41.

8. Meléndez, L. Microambiente, Cantidad de Esporas En El Aire e Incidencia Del Hongo *Miniliopthora roreri* (Cif & Par). Evans et al. Bajo Tres Sistemas de Manejo de Sombra Leguminosas En Cacao (Theobroma Cacao). Tesis de maestria, CATIE: Costa Rica, 1993.

9. Ortega Andrade, S.; Páez, G.T.; Feria, T.P.; Muñoz, J. Climate change and the risk of spread of the fungus from the high mortality of *Theobroma cocoa* in Latin America. *Neotrop. Biodivers.* **2017**, *3*, 30–40, doi:10.1080/23766808.2016.1266072.

10. Sánchez Mora, F.D.; Garcés Fiallos, F.R. *Moniliophthora roreri* (Cif y Par) Evans et al. in the crop of cocoa. *Sci. agropecu.* **2012**, 249–258, doi:10.17268/sci.agropecu.2012.03.06.

11. Leandro-Muñoz, M. Efecto de los factores macro y microclimáticas y las características productivas del cacao sobre la epidemiología de la moniliasis, CaATIE: Turrialba, 2011.

12. Zhang, Z.; Zhu, Z.; Ma, Z.; Li, H. A Molecular Mechanism of Azoxystrobin Resistance in *Penicillium digitatum* UV Mutants and a PCR-Based Assay for Detection of Azoxystrobin-Resistant Strains in Packing- or Store-House Isolates. *Int. J. Food Microbiol.* **2009**, *131*, 157–161, doi:10.1016/j.ijfoodmicro.2009.02.015.

13. Díaz-Valderrama, J.R.; Aime, M.C. The Cacao Pathogen *Moniliophthora roreri* (Marasmiaceae) Produces Rhexolytic Thallic Conidia and Their Size Is Influenced by Nuclear Condition. *Mycoscience* **2016**, *57*, 208–216, doi:10.1016/j.myc.2016.01.004.

14. Úrbez-Torres, J.R.; Battany, M.; Bettiga, L.J.; Gispert, C.; McGourty, G.; Roncoroni, J.; Smith, R.J.; Verdegaal, P.; Gubler, W.D. *Botryosphaeriaceae* Species Spore-Trapping Studies in California Vineyards. *Plant Dis.* **2010**, *94*, 717–724, doi:10.1094/PDIS-94-6-0717.

15. Bailey, B.A.; Ali, S.S.; Strem, M.D.; Meinhardt, L.W. Morphological Variants of *Moniliophthora roreri* on Artificial Media and the Biotroph/Necrotroph Shift. *Fungal Biol.* **2018**, *122*, 701–716, doi:10.1016/j.funbio.2018.03.003.

16. Schweigkofler, W.; O'Donnell, K.; Garbelotto, M. Detection and Quantification of Airborne Conidia of *Fusarium circinatum*, the Causal Agent of Pine Pitch Canker, from Two California Sites by Using a Real-Time PCR Approach Combined with a Simple Spore Trapping Method. *Appl. Environ. Microbiol.* **2004**, *70*, 3512–3520, doi:10.1128/AEM.70.6.3512-3520.2004.

17. Quesada, T.; Hughes, J.; Smith, K.; Shin, K.; James, P.; Smith, J. A Low-Cost Spore Trap Allows Collection and Real-Time PCR Quantification of Airborne *Fusarium circinatum* Spores. *Forests* **2018**, *9*, 586, doi:10.3390/f9100586.

18. Dvořák, M.; Janoš, P.; Botella, L.; Rotková, G.; Zas, R. Spore Dispersal Patterns of *Fusarium circinatum* on an Infested Monterey Pine Forest in North-Western Spain. *Forests* **2017**, *8*, 432, doi:10.3390/f8110432.

19. Chandelier, A.; Helson, M.; Dvorak, M.; Gischer, F. Detection and Quantification of Airborne Inoculum of *Hymenoscyphus pseudoalbidus* Using Real-Time PCR Assays. *Plant Pathol* **2014**, *63*, 1296–1305, doi:10.1111/ppa.12218.

20. Raja, H.A.; Miller, A.N.; Pearce, C.J.; Oberlies, N.H. Fungal Identification Using Molecular Tools: A Primer for the Natural Products Research Community. *J. Nat. Prod.* **2017**, *80*, 756–770, doi:10.1021/acs.jnatprod.6b01085.

21. Rausch, T.; Fritz, M.H.-Y.; Untergasser, A.; Benes, V. Tracy: Basecalling, Alignment, Assembly and Deconvolution of Sanger Chromatogram Trace Files. *BMC Genomics* **2020**, *21*, 230, doi:10.1186/s12864-020-6635-8.

22. Kralik, P.; Ricchi, M. A Basic Guide to Real Time PCR in Microbial Diagnostics: Definitions, Parameters, and Everything. *Front. Microbiol.* **2017**, *8*, doi:10.3389/fmicb.2017.00108.

23. Wickham, H. *Ggplot2: Elegant Graphics for Data Analysis*; Springer-Verlag New York, 2016; ISBN 978-3-319-24277-4.

24. R Development Core Team *Language and Environment for Statistical Computing: Reference Index*; R Foundation for Statistical Computing: Vienna, 2021; ISBN 978-3-900051-07-5.

25. Ruijter, J.M.; Barnewall, R.J.; Marsh, I.B.; Szentirmay, A.N.; Quinn, J.C.; van Houdt, R.; Gunst, Q.D.; van den Hoff, M.J.B. Efficiency Correction Is Required for Accurate Quantitative PCR Analysis and Reporting. *Clin. Chem.* **2021**, *67*, 829–842, doi:10.1093/clinchem/hvab052.

26. Bustin, S.A.; Benes, V.; Garson, J.A.; Hellemans, J.; Huggett, J.; Kubista, M.; Mueller, R.; Nolan, T.; Pfaffl, M.W.; Shipley, G.L.; et al. The MIQE Guidelines: Minimum Information for Publication of Quantitative Real-Time PCR Experiments. *Clin. Chem* **2009**, *55*, 611–622, doi:10.1373/clinchem.2008.112797.

27. Bates, D.; Mächler, M.; Bolker, B.; Walker, S. Fitting Linear Mixed-Effects Models Using Lme4. *J. Stat. Softw.* **2015**, *67*, 1–48, doi:10.18637/jss.v067.i01.

28. Lüdecke, D. SjPlot: Data Visualization for Statistics in Social Science 2021.

29. Abdullah, A.S.; Turo, C.; Moffat, C.S.; Lopez-Ruiz, F.J.; Gibberd, M.R.; Hamblin, J.; Zerihun, A. Real-Time PCR for Diagnosing and Quantifying Co-Infection by Two Globally Distributed Fungal Pathogens of Wheat. *Front. Plant Sci.* **2018**, *9*, 1086, doi:10.3389/fpls.2018.01086.

30. *Cacao Diseases: A History of Old Enemies and New Encounters*; Bailey, B.A., Meinhardt, L.W., Eds.; Springer: Cham Heidelberg New York, 2016; ISBN 978-3-319-24787-8.

31. Klosterman, S.J.; Anchieta, A.; McRoberts, N.; Koike, S.T.; Subbarao, K.V.; Voglmayr, H.; Choi, Y.-J.; Thines, M.; Martin, F.N. Coupling Spore Traps and Quantitative PCR Assays for Detection of the Downy Mildew Pathogens of Spinach (*Peronospora effusa*) and Beet (*P. schachtii*). *Phytopathology* **2014**, *104*, 1349–1359, doi:10.1094/PHYTO-02-14-0054-R.

32. Brankatschk, R.; Bodenhausen, N.; Zeyer, J.; Bürgmann, H. Simple Absolute Quantification Method Correcting for Quantitative PCR Efficiency Variations for Microbial Community Samples. *Appl. Environ. Microbiol.* **2012**, *78*, 4481–4489, doi:10.1128/AEM.07878-11.

33. Su'udi, M.; Park, J.-M.; Kang, W.-R.; Park, S.-R.; Hwang, D.-J.; Ahn, I.-P. Quantification of Rice Brown Leaf Spot through Taqman Real-Time PCR Specific to the Unigene Encoding *Cochliobolus miyabeanus* SCYTALONE DEHYDRATASE1 Involved in Fungal Melanin Biosynthesis. *J Microbiol.* **2012**, *50*, 947–954, doi:10.1007/s12275-012-2538-y.

34. Kennedy, R.; Wakeham, A.J.; Byrne, K.G.; Meyer, U.M.; Dewey, F.M. A New Method To Monitor Airborne Inoculum of the Fungal Plant Pathogens *Mycosphaerella brassicicola* and *Botrytis cinerea*. *Appl Environ Microbiol* **2000**, *66*, 2996–3003, doi:10.1128/AEM.66.7.2996-3003.2000.